Development 130, 507-518

doi:10.1242/dev.00241

Cell autonomous requirement for PDGFRα in populations of cranial and cardiac neural crest cells

Michelle D. Tallquist*,† and Philippe Soriano

Program in Developmental Biology and Division of Basic Sciences, Fred Hutchinson Cancer Research Center, 1100 Fairview Avenue North, Seattle, WA 98109, USA

*Present address: Department of Molecular Biology, University of Texas Southwestern Medical Center, 5323 Harry Hines Blvd, Dallas, TX 75390-9148, USA
†Author for correspondence (e-mail: michelle.tallquist@utsouthwestern.edu)

Accepted 31 October 2002

SUMMARY

Cardiac and cephalic neural crest cells (NCCs) are essential components of the craniofacial and aortic arch mesenchyme. Genetic disruption of the platelet-derived growth factor receptor α (PDGFRα) results in defects in multiple tissues in the mouse, including neural crest derivatives contributing to the frontonasal process and the aortic arch. Using chimeric analysis, we show that loss of the receptor in NCCs renders them inefficient at contributing to the cranial mesenchyme. Conditional gene ablation in NCCs results in neonatal lethality because of aortic arch defects and a severely cleft palate. The conotruncal defects are first observed at E11.5 and are consistent with aberrant NCC development in the third, fourth and sixth branchial arches, while the bone malformations present in the frontonasal process and skull coincide with defects of NCCs from the first to third branchial arches. Changes in cell proliferation, migration, or survival were not observed in PDGFRα NCC conditional embryos, suggesting that the PDGFRα may play a role in a later stage of NCC development. Our results demonstrate that the PDGFRα plays an essential, cell-autonomous role in the development of cardiac and cephalic NCCs and provides a model for the study of aberrant NCC development.

Key words: Chimeric analysis, Cre-loxP recombination, Neural crest, PDGF receptor, Mouse

INTRODUCTION

Neural crest cells (NCCs) are a migratory population of cells that participate in the formation of a variety of tissues, including craniofacial structures, great arteries and the peripheral nervous system. This versatile lineage of cells is patterned at four overlapping axial levels of the embryo. NCCs emanating from the anterior neural tube (cranial neural crest) differentiate into a variety of bone, cartilage, cranial ganglia and connective tissue of the head and neck, while NCCs arising from the more caudal regions (cardiac neural crest) contribute to the vascular smooth muscle cells (VSMC) of the aortic arch. Cells of the remaining two populations (trunk and vagal neural crest) contribute to the trunk peripheral nervous system and the enteric nervous system. Targeted mutations in mice have revealed a plethora of genes that play a role in the formation of cranial and cardiac NCC derivatives (Maschhoff and Baldwin, 2000), reinforcing the idea that a complex set of environmental and intrinsic factors determine the fate of these cells. Interestingly, many of these disruptions lead to defects in both cardiac and cranial NCCs and are linked to a diverse set of signaling molecules, including endothelins, retinoids, BMPs, Wnts and PDGFs. Although these pathways have been implicated in the formation of the NCC derivatives, little is known about how they direct NCC migration and/or differentiation.

It has been proposed that signaling through the PDGFRα is required for the development of non-neuronal neural crest of cephalic and cardiac origin. These findings were first identified in the naturally occurring mouse mutant patch (*Ph*) (Grüneberg and Truslove, 1960; Morrison-Graham et al., 1992; Smith et al., 1991; Stephenson et al., 1991), which carries a deletion encompassing the PDGFRα gene. *Ph/+* heterozygotes exhibit defects in melanocyte development and *Ph/Ph* embryos exhibit recessive defects in the axial skeleton, cardiac, and cranial neural crest. Targeted disruption of the PDGFRα locus has demonstrated that *Pdgfra* and *Ph* mutations share nearly identical phenotypes with the exception of the heterozygous melanocyte defect (Soriano, 1997), although deficiencies in melanocyte development have been observed in chimeric animals using null or hypomorphic PDGFRα alleles (Klinghoffer et al., 2002).

More recently, several other affected tissues have been shown to require PDGFRα signaling, including kidney interstitial fibroblasts, testes Leydig cells and intestinal villus cells (reviewed by Betsholtz et al., 2001). Despite the fact that many studies have uncovered specific cellular roles for PDGFRα, very little is known about the mechanism of action

of PDGFRα in vivo. The analysis of biological function of PDGFRα during development is complicated because many cell types express the receptor, which results in variable phenotypes and early lethality. The expression pattern of the PDGFRα during embryogenesis is diverse and extensive. At E6.5, PDGFRα mRNA is expressed in visceral extra-embryonic endoderm. After gastrulation the receptor mRNA can be seen in many areas of mesenchyme, including the somites, limb buds and branchial arches (Orr-Urtreger et al., 1992; Orr-Urtreger and Lonai, 1992; Schatteman et al., 1992). Less than one-third of the mutant embryos survive beyond E11.5 on the C57BL/6 background, making analysis of the NCC phenotypes difficult (M. D. T., unpublished). In the NCC population, the PDGFRα is expressed in a broad diffuse pattern that is synonymous with regions defined for cranial and cardiac NCCs (Orr-Urtreger et al., 1992; Orr-Urtreger and Lonai, 1992; Schatteman et al., 1992; Takakura et al., 1997; Zhang et al., 1998). The early embryonic lethality and broad expression pattern of the PDGFRα make elucidation of cell autonomous functions of the receptor in NCCs very challenging.

To investigate potential cell autonomous requirements for PDGFRα signaling in cranial and cardiac NCCs, we have generated chimeric or mosaic embryos. Traditional chimeras were generated by mixing mutant and wild-type cells in pre-implantation embryos. In these chimeras, we found a strong selection for cells bearing the PDGFRα in several mesenchymal cell populations, including limb bud, somite and branchial arches. To further investigate the role of the PDGFRα, we performed tissue-specific gene ablation using Cre/loxP recombination exclusively in the NCC lineage. We found that loss of PDGFRα in NCCs results in craniofacial and aortic arch defects, while many of the other phenotypes are alleviated. From these analyses, we have determined that PDGFRα is directly required in both cardiac and cranial NCCs, and we have further characterized the phenotypes associated with these particular cell types.

MATERIALS AND METHODS

Chimeric analysis

Homozygous PDGFRα-null embryonic stem (ES) cells were generated de novo from blastocysts of heterozygous PDGFRα (αR4) mice (Soriano, 1997) on a 129S4 congenic background. Two lines of PDGFRα-null ES cells were generated, and both cell lines yielded similar results. The presence of the null allele was verified by Southern blotting. Chimeric embryos were generated by injecting the PDGFRα-null ES cells into ROSA26 heterozygous blastocysts, which express *lacZ* constitutively (Zambrowicz et al., 1997). In addition, one ES cell line was tagged using a β-galactosidase-neo fusion (βgeo) expression cassette targeted to the ROSA26 locus. For this purpose, the neo cassette was removed from the PDGFRα locus by transient expression with PGKCrebpA, and the cells were electroporated with pROSA26-βgeo, in which βgeo has been introduced at the unique *Xba*I cloning site of pROSA26-1 (Soriano, 1999). After electroporation, approx. one third of the ES cell clones were shown to have undergone homologous recombination by PCR and Southern analysis as described previously (Soriano, 1999). One *Pdgfra*$^{-/-}$ R26-βgeo-tagged subclone was then injected into wild-type blastocysts. For all chimeras generated, embryos were isolated, fixed, stained for β-galactosidase activity and processed for histology. The ES cell contribution was estimated by β-galactosidase staining of histological sections of the indicated tissue.

Table 1. Distribution of *Pdgfra*-null cells in branchial arch mesenchyme of chimeric animals

Chimera number	Mutant phenotype	Tissue				
		BA I	BA II	BA III	BA IV-VI	DRG
CH1	+++	100	100	100	100	100
CH2	++	90	100	100	100	100
CH3	++	80	80	na	na	100
CH4	+	60	40	50	na	80
CH5	–	30	30	20	20	90
CH6	+	10	10	80	90	40
CH7	++	40	20	10	na	80
CH8	–	10	10	10	10	50
CH9	–	0	10	40	na	80
CH10	–	30	30	30	na	50
CH11	–	0	20	20	20	60

The contribution of mutant cells was estimated on β-galactosidase-stained sections from the dorsal root ganglia (DRG), which displayed no bias for cells of wild-type or *Pdgfra*$^{-/-}$ genotype. Therefore, we used the DRG as the indicator tissue for determining the overall contribution of mutant cells in the chimeras.

Values in table are estimations only and are not intended to carry statistical significance. For the branchial arch values, we could not make a distinction between paraxial mesoderm-derived cells and neural crest-derived cells; therefore, the values reflect both cell populations. BA, branchial arch; DRG, dorsal root ganglia.

Mutant column indicates similarity of phenotype when compared with *Pdgfra*-null E10 embryos. +++, similar to most severe phenotypes (wavy neural tube, dilated pericardium, growth retarded, blebbing); ++, growth retarded, blebbing; +, growth retarded; –, no phenotype observed; na, embryos had not developed to a stage where these branchial arches could be examined thoroughly.

Values presented in Table 1 are approximations of β-galactosidase staining.

Mice and genotyping

The targeting construct for the PDGFRα floxed allele was generated using genomic DNA that has been previously described (Soriano, 1997). A *loxP* site was inserted into the *Bam*HI site located upstream of the exon encoding the signal peptide. Pgk-neo *loxP* was inserted at the *Sma*I site. Wnt1Cre transgenic mice (Danielian et al., 1998) were kindly provided by Andy McMahon (Harvard University). ROSA26R Cre reporter mice expressing *lacZ* conditionally have been described previously (Soriano, 1999). All mice were maintained on mixed genetic backgrounds, except for mice bearing the null allele, which were either congenic on C57BL/6 or on 129S4. PDGFRα^{fl} and null alleles were genotyped using PCR primers described for the *Pdgfra*-null allele (Soriano, 1997). The Wnt1Cre transgene was detected by Southern blot analysis for Cre.

Flow cytometry

Flow cytometric data analysis (FACScan, Becton Dickinson, Palo Alto, CA) was used to determine the cell-surface expression of PDGFRα in branchial arch mesenchyme. E10.5 embryos were isolated and the branchial arch region dissected using tungsten needles. The arch tissue was dissociated using 1 mg/ml dispase (Boehringer-Mannheim) in PBS for 10 minutes at 37°C. Single cell suspension was filtered through nylon mesh. APA5 (Research Diagnostics, Flanders, NJ), a rat monoclonal antibody that reacts with the murine PDGFRα, was used at a 1:200 dilution. We used goat anti Rat IgG conjugated to phycoerythrin (Jackson Immunoresearch, West Grove, PA) as secondary antibody.

Resin injections

Resin injections were performed using Batson's #17 Plastic Replica and Corrosion Kit, (Polysciences; Warrington, PA). E18.5 embryos

were isolated by cesarian section. The thoracic cavity was opened and resin injected into the left or right ventricle using a glass drawn pipette. Resin was allowed to harden overnight at 4°C and tissue was then macerated for 1-2 hours at 50°C using Maceration Solution (Polysciences, Warrington, PA).

Intracardiac ink injection

Embryos were collected at E9.5-11.5 and India ink was injected into the left ventricle using a finely drawn glass pipette. The embryos were then immediately fixed in either 4% paraformaldehyde or methyl Carnoy's. Embryos were cleared in benzyl alchol:benzyl benzoate and photographed. Vessels were scored for presence, absence and thickness.

Immunohistochemistry and TUNEL analysis

Tissues were fixed in 4% paraformaldehyde, sectioned, deparaffinized and rehydrated. For immunohistochemistry, endogenous peroxidase activity was quenched using 3%H_20_2/10% methanol in PBS at for 30 minutes. Antigens were revealed using 2N HCl at room temperature for 45 minutes followed by a 0.1% trypsin incubation at 37°C for 20 minutes. Antibodies against α smooth muscle actin (1:10000; clone 1A4, Sigma), PECAM (1:200; clone MEC 13.3, Pharmingen) and phospho-histone H3 (1:200; #06-570, Upstate Biotech) were incubated for 1 hour at room temperature and detected using the appropriate secondary antibody. The HRP reaction was performed using the Vectastain (Vector Labs) ABC and DAB kits. The TUNEL protocol was as described by Gavrieli et al. (Gavrieli et al., 1992). Briefly, nuclear proteins were stripped with 20 μg/ml proteinase K in PBS for 10 minutes at room temperature. Sections were then washed with TdT buffer (30mM Tris pH 7.2/140 mM cacodylic acid/1mM $CoCl_2$). TdT reaction was accomplished in TdT buffer with 0.3 units/μl TdT (Pharmacia) and 7.5 μM biotinylated-14-dATP (Gibco/BRL) for 1 hour at 37°C. The Vectastain ABC and DAB kits (Vector Labs) were used to visualize the incorporated ATP.

RESULTS

Chimeric analysis

Although it has been suggested that the PDGFRα plays a role in cranial and cardiac neural crest development, the pleiotropic phenotypes of the *Ph*- and *Pdgfra*-null embryos has prohibited the proof of a cell-autonomous requirement. We have used chimeric analysis to address this question. Multiple studies have shown that this technique can be used to identify cell types that are dependent on the gene of interest (reviewed by Nagy and Rossant, 2001; Rossant and Spence, 1998). Chimeras were generated either by injecting the *Pdgfra*-null ES cells into ROSA26 blastocysts, or *Pdgfra*-null β-galactosidase-tagged ES cells into wild-type blastocysts (see Materials and methods). ROSA26 derived cells express β-galactosidase ubiquitously and provide a means of distinguishing cells of different genotypes (Friedrich and Soriano, 1991).

Cranial and cardiac crest initiate migration at day 8 (E8); therefore, we examined chimeric embryos at day 9 and 10 of gestation. ES cell contribution to these chimeras ranged from 0-100%, as judged by an estimation of β-galactosidase-negative cell contribution to the dorsal root ganglia (DRG), where there was no selection bias for cells of different genotypes. We were able to obtain extensively mutant chimeras from both ES cell lines, but chimeras with more than 50% mutant ES cell contribution were phenotypically abnormal and often indistinguishable from *Pdgfra*-null embryos (Fig. 1A-E; Table 1). The phenotypic abnormalities included growth retardation, dilated pericardium, surface ectoderm blebbing, wavy neural tube and hypoplastic branchial arches. In fact, we recovered a chimera that was ~100% ES cell derived (based on PCR and β-galactosidase staining). The phenotype appeared identical to that observed in *Pdgfra*-null embryos. Because injected ES cells contribute primarily to epiblast derivatives (Beddington and Robertson, 1989), these data suggest that the phenotypes at E9.5-10.5 are due to defects in loss of PDGRα from the embryo and/or extra-embryonic mesoderm and not likely to be due to defects in other extra-embryonic tissues.

Analysis of the chimeras in wholemount and sections revealed a striking selection against PDGFRα-positive cells in several areas of mesenchyme (Fig. 1). These included the limb bud progress zone, branchial arches and sclerotome (Table 1 and data not shown). Fig. 1F is an example of a section through a chimera that contains a significant proportion of *Pdgfra*$^{-/-}$ cells (70-100% in the neural tube) while much of the mesenchyme is wild-type derived. In forelimb buds, we observed progress zones that were almost exclusively composed of wild-type cells, while the adjacent surface ectoderm was populated mostly by *Pdgfra*$^{-/-}$ cells (Fig. 1F, inset). In the less mature hindlimb bud, wild-type and mutant cells are mixed in the more proximal region, but in the distal zone there is a concentration of wild-type cells abutting the ligand-expressing surface ectoderm.

A similar pattern of selection was seen when we examined neural crest-derived head and branchial arch mesenchyme. Again, *Pdgfra*$^{-/-}$ cells contribute to the ectodermal epithelium and the paraxial mesoderm-derived core of the branchial arches (Fig. 1G-J) (data not shown), but neural crest-derived ectomesenchyme is almost exclusively composed of wild-type cells. Analysis of proliferation in the branchial arches of these chimeras using anti-phosphohistone 3 antibody or BrdU labeling did not yield definitive results because the number of null cells available for analysis in the tissues of interest was limited, and the number of proliferating null cells was negligible. Nonetheless, the strong selection against the null cells in areas of proliferating mesenchyme of the limb and NCC-derived ectomesenchyme suggests a cell autonomous requirement for PDGFRα in these tissues.

Conditional analysis of PDGFRα in neural crest

We wanted to study further the role of PDGFRα in the neural crest lineage, but because many of the high percent chimeras possessed the *Pdgfra*$^{-/-}$ phenotypes, we chose to analyze PDGFRα signaling in the NCCs by conditional gene ablation analysis. Fig. 2A depicts the construction of the mutant allele (PDGFRα^{fl}) flanked by lox sites (floxed). In the presence of Cre recombinase, the second and third exon of the *Pdgfra* gene as well as the neo cassette will be removed, resulting in a null allele identical to the one previously described (Soriano, 1997). While homozygous mice bearing this floxed allele are viable with no overt phenotype, the presence of the *Pgk-neo loxP* cassette apparently interferes with gene expression. This result was revealed when we crossed mice bearing the null allele to PDGFRα$^{fl/fl}$. From seven litters, no transheterozygotes were obtained at the time of weaning. These data suggest that transheterozygotes of the *Pdgfra*-null allele and floxed allele are inviable due to reduced levels of receptor expression.

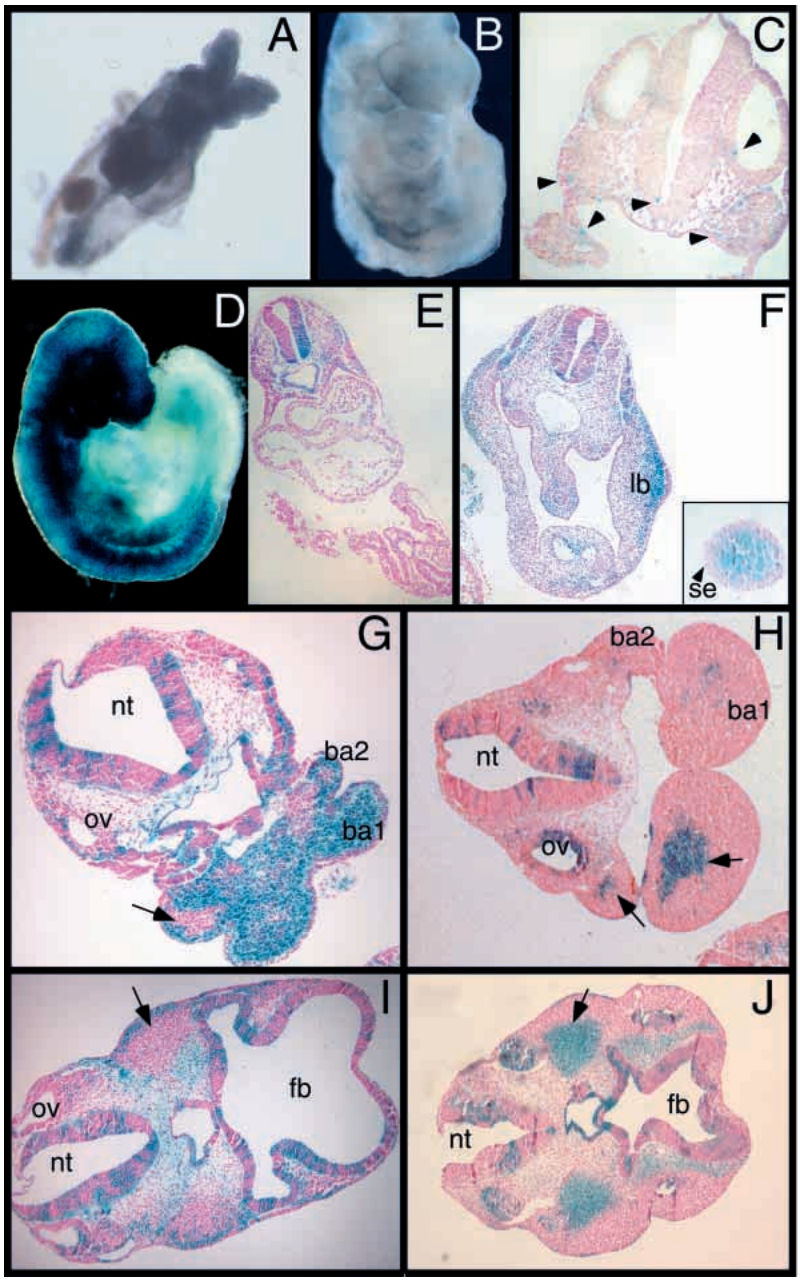

Fig. 1. *Pdgfra*$^{-/-}$ cells contribute minimally to limb bud and cranial ectomesenchyme. (A-G,I) *Pdgfra*$^{-/-}$ ES cells injected into ROSA26$^{+/-}$ blastocysts; chimeras after staining for β-galactosidase activity. (A-E) E10.5 chimeras that contain a high percentage of *Pdgfra*$^{-/-}$ cells phenocopy *Pdgfra*$^{-/-}$ embryos (A, CH1; B,C, CH2; D,E, CH3; see Table 1). (C,E) Transverse sections through chimeras shown in B and D at the cranial and cardiac crest level, respectively. (F) Transverse section through hindlimb bud of 50% mutant cell derived chimera (CH8). Inset shows a section through forelimb bud with predominantly *Pdgfra*$^{-/-}$ contribution to surface ectoderm (arrowhead) and wild-type contribution to the mesenchyme. (G,I) Transverse sections of branchial arches and head mesenchyme from chimeras generated by injection of *Pdgfra*$^{-/-}$ ES cells into ROSA26$^{+/-}$ blastocysts (CH11). (H,J) Transverse sections through similar regions to those in G and I for chimeras made by injection of *Pdgfra*$^{-/-}$; ROSA26$^{+/-}$ ES cells into wild-type blastocysts (CH10). nt, neural tube; se, surface ectoderm; lb, limb bud; ov, otic vesicle; ba1, branchial arch 1; ba2, branchial arch 2; fb, forebrain. Arrows in G-J indicate regions of mesoderm-derived muscle progenitors. Arrowheads in C indicate location of occasional wild-type cells.

Because the floxed allele is hypomorphic, we have used both the homozygous floxed mice (PDGFRα$^{fl/fl}$) and Wnt1Cre^{+}; PDGFRα$^{fl/+}$ as littermate controls. We have observed no craniofacial nor cardiac NCC defects in PDGFRα$^{fl/fl}$ embryos or Wnt1Cre^{+}; PDGFRα$^{fl/+}$ mice.

To investigate specifically the role of the PDGFRα in NCCs, we crossed the PDGFRα conditional allele to the Wnt1Cre mouse line. In this line, the Cre recombinase is expressed in the dorsal neural tube as early as embryonic day 8 (E8), and therefore in the presumptive neural crest. Several studies have used the transgenic Wnt1Cre line in combination with the ROSA26 Cre reporter line (where β-galactosidase is expressed upon recombination by Cre) as a lineage marker for NCCs (Chai et al., 2000; Echelard et al., 1994; Jiang et al., 2000); Cre is expressed at the correct time and place to delete the PDGFRα from the neural crest (Fig. 2C,D). We determined the extent of tissue-specific PDGFRα gene ablation in several ways. First, Southern blot analysis verified that the deleted floxed allele resulted in the expected genetic rearrangement in head mesenchyme (Fig. 2B). Second, the distribution of tissues with Cre recombination was investigated using the ROSA26R Cre reporter mouse. In both wild-type and PDGFRα$^{fl/fl}$;Wnt1Cre^{+} embryos (also referred to as NCC conditionals), the pattern of Cre activity follows the localization of NCC derivatives (Fig. 2C,D). In addition, it appears that at E9 many of the cells express β-galactosidase, suggesting that most cells of neural crest origin exhibit recombination of the *loxP* flanked DNA. Therefore at this time point, few if any cells have escaped Cre recombination activity and thus have lost PDGFRα expression and this is further illustrated by the findings from protein expression. As a final approach to examining the efficiency of the Cre recombinase, we measured PDGFRα protein expression by flow cytometry. Fig. 2E indicates that as early as E10.5, PDGFRα expression in the mesenchyme of the branchial arches has dropped below detection limits. These results indicate that the Wnt1-driven Cre is expressed in the appropriate tissues, at the correct time, and at sufficient levels to render NCC derivatives void of PDGFRα protein expression.

To determine the outcome of loss of PDGFRα in NCCs, we established matings of PDGFRα$^{fl/+}$;Wnt1Cre^{+} males to PDGFRα$^{fl/fl}$ females. No viable PDGFRα$^{fl/fl}$;Wnt1Cre^{+} neonates were obtained from 181 offspring. In contrast to PDGFRα$^{-/-}$ embryos which are resorbed several days before birth, several NCC conditional newborns were found dead with a foreshortened snout, a sagittal median cleft, and often a midline hemorrhage. These external defects were accompanied by a cleft palate (Fig. 3A-B). While the extent of the frontonasal fusion

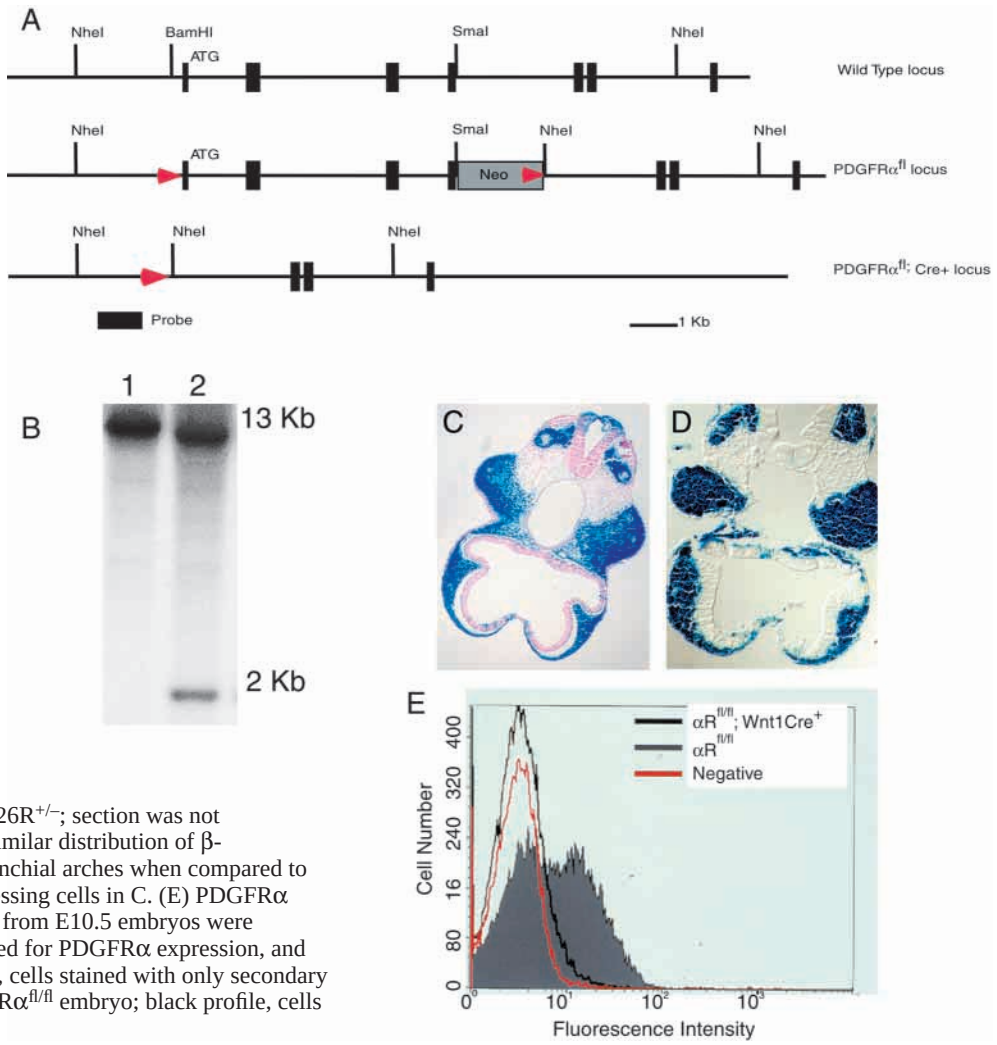

Fig. 2. PDGFRα conditional allele and analysis of Cre efficiency. (A) The wild-type PDGFRα locus, the targeted floxed allele and the resulting allele after Cre-mediated inactivation of the PDGFRα. The deleted region of genomic DNA in the fl allele is identical to that deleted in the PDGFRα null allele αR4 (Soriano, 1997). Black boxes represent exons. The floxed allele contains the neo cassette (gray box). Red arrowheads represent loxP sites, and the small black rectangle represents the probe used in Southern blot analysis. (B) Southern analysis of tissues from E13.5 PDGFRα$^{fl/fl}$; Wnt1Cre^{+} embryos. Genomic DNA was digested with *Nhe*I and probed with fragment indicated in A. Lane 1, DNA from yolk sac; lane 2, DNA from cranial tissues. (C,D) Transverse sections through first branchial arch region of E9 embryos stained for β-galactosidase activity. (C) ROSA26R$^{+/-}$; Wnt1Cre^{+}; section was counterstained with nuclear Fast Red. (D) PDGFRα$^{fl/fl}$;Wnt1Cre^{+};ROSA26R$^{+/-}$; section was not counterstained. Note that D contains a similar distribution of β-galactosidase-expressing cells in the branchial arches when compared to the distribution of β-galactosidase-expressing cells in C. (E) PDGFRα cell-surface expression histogram. Cells from E10.5 embryos were isolated from the branchial arches, stained for PDGFRα expression, and analyzed by flow cytometry. Red profile, cells stained with only secondary antibody; gray profile, cells from PDGFRα$^{fl/fl}$ embryo; black profile, cells from PDGFRα$^{fl/fl}$;Wnt1Cre embryo.

varied between NCC conditional mice, the palatal defect remained consistent with complete failure of the shelves to fuse. This phenotype was fully penetrant and never observed in PDGFRα$^{fl/fl}$ or PDGFRα$^{fl/+}$; Wnt1Cre^{+} mice. The phenotype of the PDGFRα NCC conditional and null embryos were compared at E13.5-15.5 (Fig. 3C,D). Fig. 3D demonstrates that the NCC conditional embryos possessed a midline facial cleft often accompanied by a hemorrhagic bleb. Even though the midline defect was always present, it rarely extended the length of the anterior mesencephalon as the clefts in the null embryos do. To study the etiology of the craniofacial defects, we examined embryos at various time points. From E8.5 to E10.5, NCC conditional embryos were indistinguishable from littermate controls. Starting at E11.5, NCC conditional embryos possessed a gap in the frontal nasal process (Fig. 4E,F). At this time point, no hemorrhaging or blebbing was evident, although by E13.5 both were observed (Fig. 3D). External examination of the embryos also showed that the subepidermal blebbing adjacent to the thoracic and lumbar vertebrae and on the flanks that is observed in *Pdgfra*-null embryos was not present in the NCC conditional embryos. To determine the extent of the phenotype similarities between the NCC conditional and null embryos, we examined histological and bone preparations. We observed no phenotypes in the other PDGFRα-dependent tissues, such as the kidney, lungs, intestines or bones of the axial skeleton (data not shown).

Craniofacial bone defects

Detailed analysis of cranial skeleton and cartilage defects in *Pdgfra*$^{-/-}$ embryos had not been possible because most embryos die before these structures have developed. Therefore, we examined the NCC conditional mutants to understand the extent of the craniofacial defects in the absence of PDGFRα signaling. NCCs from the branchial arches contribute to the bony and cartilaginous structures of the cranium in the mouse (Trainor and Tam, 1995), and we analyzed these structures using Alcian Blue/Alizarin Red staining from E17.5-P1 embryos. Grüneberg and Truslove (Grüneberg and Truslove, 1960) noted that the cranial cavity of *Ph*/+ mice was shorter and broader than those measured in wild-type skulls. We compared the skulls of PDGFRα$^{fl/fl}$;Wnt1Cre^{+} to PDGFRα$^{fl/fl}$ embryos at E17.5 and observed that the NCC conditional skulls were shortened 8±1%. All the NCC conditional mutants exhibited a cleft palate where the palatine and maxillary shelves failed to fuse. Although the midline frontal nasal clefting was always present, the defect ranged in severity from

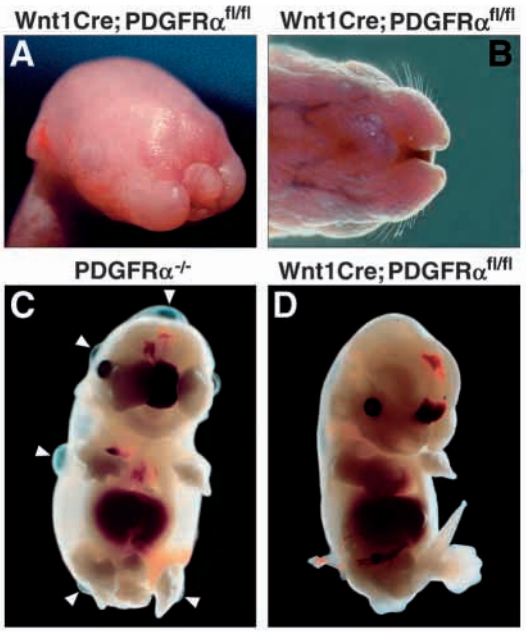

Fig. 3. PDGFRα$^{fl\Delta/fl\Delta}$; Wnt1Cre^{+} and *Pdgfra*$^{-/-}$ neonates and embryos. (A,B) External appearance of NCC conditional mutants after birth. Frontal and ventral view, respectively. The embryo in A is albino; therefore, it lacks pigment in the retinal epithelium. (C) E14.5, PDGFRα embryo has extensive blebbing (arrowheads) and edema. (D) E13.5, PDGFRα$^{fl/fl}$;Wnt1Cre^{+} possesses the midline facial hemorrhage.

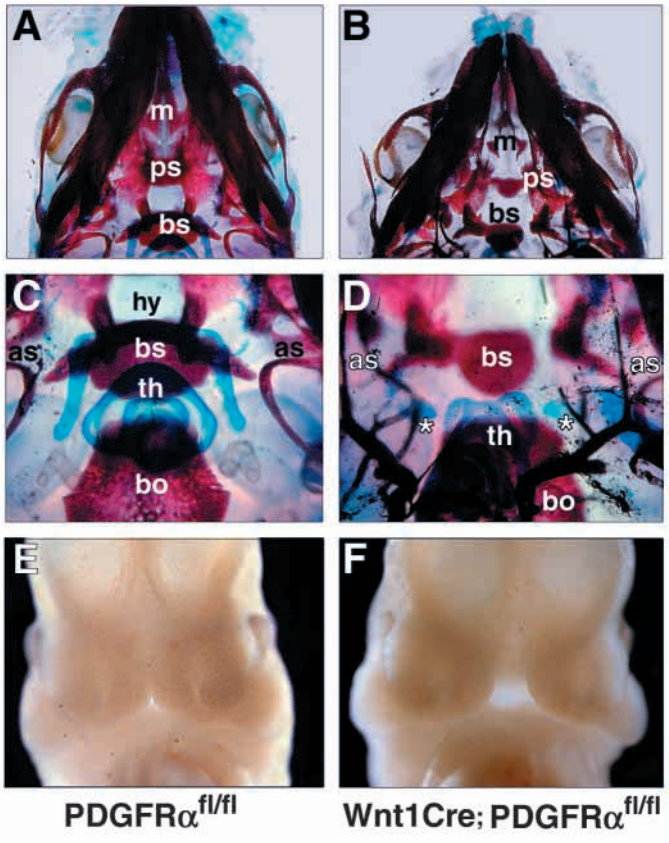

Fig. 4. Cranial and frontonasal defects in PDGFRα$^{fl/fl}$;Wnt1Cre embryos. (A-D) Ventral views of skeletal preparations from E17.5 wild type and NCC conditional embryos. (C,D) The mandible was removed for visualization of the palate. as, alisphenoid bone; bo, basioccipital bone; bs, basisphenoid bone; h, hyoid bone; m, maxilla; ps, palatal shelf; th, thyroid cartilage. *Cartilage remnants potentially from the hyoid horns. Note blood vessels prominent in D because of filling with India ink. (E,F) Frontal view of E11.5 PDGFRα$^{fl/fl}$ and PDGFRα$^{fl/fl}$; Wnt1Cre^{+} embryos, respectively. The frontonasal masses fail to meet at the midline.

a full, blood-filled, cleft spanning the anterior forebrain to the frontal nasal process to a small hemorrhage overlying the nasal cavity. Even in the less severe examples, the nasal capsule and the overlying frontal and nasal bones were lacking or failed to fuse. In many embryos the vomer and nasal septum were malformed (data not shown). Defects including rudimentary structures and incomplete ossification were observed in many other NCC-derived bones, including the basosphenoid, presphenoid and alisphenoid bones (Fig. 4A-D and data not shown). The hyoid bone derived from both the second and third arches was either absent or fused to the thyroid cartilage in all mutants examined (3/3). In one instance, only the horns of the hyoid bone were observed (Fig. 4D). In contrast to these defects, other cranial neural crest derivatives were very similar to wild type. The mandible, tympanic ring and styloid process were unperturbed in the NCC conditional embryos. Thus, the PDGFRα is required for proper formation of some but not all cranial NCC structures.

In the mouse, cranial NCCs arise from the dorsal neural tube before it closes and must migrate to the anterior facial primordium, where they contribute to the frontonasal prominence and the pharyngeal arches (Osumi-Yamashita et al., 1994; Trainor and Tam, 1995). It has been proposed that PDGFRα is required for proliferation of multiple progenitor cell types and loss of this signal results in insufficient differentiated progeny (Betsholtz et al., 2001). To investigate if the cranial NCC defects observed in the NCC conditional embryos were caused by a lack of proliferation, we performed immunohistochemistry for phosphohistone 3 on the craniofacial mesenchyme at several time points. Fig. 5 illustrates a typical result at E11.5. The numbers of proliferating cells in the ectomesenchyme are the same in wild-type and mutant embryos. These data suggest that the craniofacial defects are not caused by a global lack of proliferation of NCC derivatives. Likewise, we observed no changes in the number of apoptotic cells, as detected by TUNEL staining (data not shown). An important point to note is that the wild-type and mutant arches are very similar in size and shape, with the major exception being the lack of fusion between the frontal nasal processes in the mutant embryo. We infer from these observations that the majority of the NCC progeny are present within the arches and that one cause of the craniofacial defects could be failure of midline fusion. There are reports that pharyngeal arches can form and be patterned in the absence of NCCs. In these studies, there were no changes in pharyngeal arch apoptosis or proliferation, even though NCCs were absent (Veitch et al., 1999; Gavalas et al., 2001). Given this information, loss of a subpopulation of NCCs may not be obvious using these two techniques.

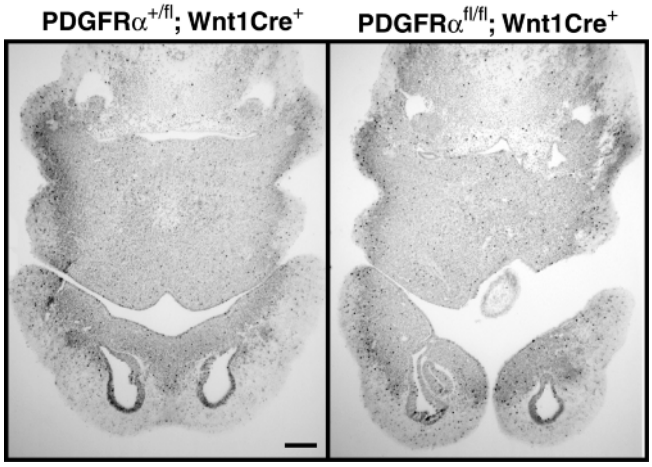

Fig. 5. Proliferation in craniofacial mesenchyme. (A,B) Transverse sections though frontal nasal process of E11.5 embryos. Punctate staining pattern indicates phosphohistone 3 positive cells. Scale bar: 200 μm.

Cardiovascular defects in PDGFRα NCC conditional embryos

Because aortic arch and thymus anomalies had been described in *Ph* mutants (Morrison-Graham et al., 1992), we examined these tissues in the PDGFRα NCC conditional embryos. A decrease in thymus size was observed at very low penetrance (three out of 32 E18.5 NCC conditional embryos; data not shown). To investigate potential aortic arch defects, corrosion casts were prepared at E18.5. In greater than 50% of the NCC conditional embryos, we identified several arch anomalies that have been associated with defects in cardiac crest. This number may be an underestimate of the embryos harboring defects, because in multiple castings there was vessel rupture and incomplete filling of the vessels. Inability to cast the vessels occurred almost exclusively in the NCC conditional embryos. A similar loss in vessel integrity was also observed in the *Ph* mutants (Schatteman et al., 1995). Fig. 6 provides examples of the range of defects observed. The most severe defect observed was persistent truncus arteriosus (PTA; Fig. 6B), which results from failure of the conotruncus to septate. Another common vascular anomaly that we observed was ectopic origin of the right subclavian artery (RSA). Frequently the RSA arose from the descending aorta (Fig. 6B,C) and in one embryo the RSA originated at the proximal pulmonary trunk (Fig. 6D). In total, we have examined 23 E17.5-E18.5 NCC conditional embryos by corrosion casting. Seven of these had incomplete filling. Ten embryos exhibited an abnormal origin of the RSA, while three of these embryos also possessed persistent truncus arteriosus. Six of the NCC conditional aortic arches appeared completely normal, with the exception of a longer innominate (two out of six). Failure of the membranous region of the ventricular septum to form is also associated with aberrant cardiac crest development (Kirby et al., 1983; Kirby and Waldo, 1990). Although ventricular septal defects (VSD) are difficult to detect in these corrosion casts because of the presence of the ductus arteriosus, resin was observed to immediately enter the right ventricle in a majority (10/16) of the NCC conditional hearts, suggesting VSD. Histological analysis of E14.5 PDGFRα NCC conditional hearts revealed a significant VSV (four out of four NCC conditional animals Fig. 7A,B). Near the apex of the heart a septum is present (Fig. 7C), demonstrating a defect in only the membranous region of the ventricular septum.

To identify the time point where the defects in the pharyngeal arches occur, we examined the arch anatomy between E9.5-11.5 with intracardiac India ink injections.

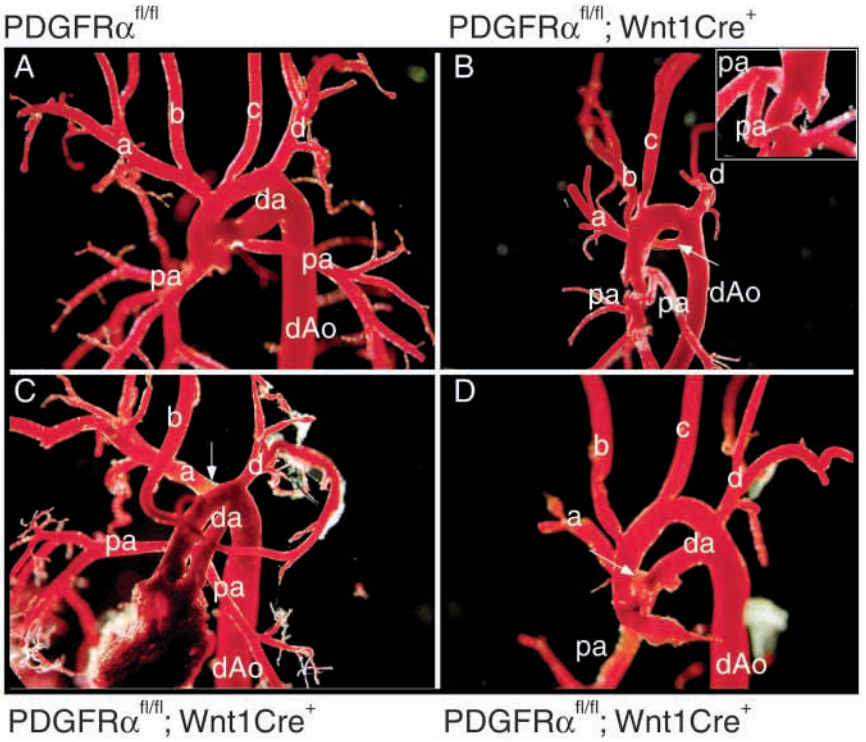

Fig. 6. Aortic arch defects in E18.5 embryos. (A) Corrosion cast of PDGFRα$^{fl/fl}$;Wnt1Cre^{-}. (B-D) PDGFRα$^{fl/fl}$;Wnt1Cre^{+} embryos. (A) Architecture of normal aortic arch where the ascending aorta has three branches. The brachiocephalic artery bifurcates into the right subclavian (a) and right common carotid (b) arteries. The next branches are the left common carotid (c) and left subclavian (d) arteries. The ductus arteriosus (da) branches off the descending aorta (dAo) with the two pulmonary arteries (pa) branching from the pulmonary trunk. (B) Persistent truncus arteriosus (PTA) and a retro-esophageal subclavian artery. Arrow indicates to the ectopic origins of the right subclavian artery. Inset in B is a higher magnification and is taken from a slightly different angle, illustrating that the pulmonary arteries are emerging from the persisting truncus arteriosus. (C) Double outlet right ventricle and retro-esophageal right subclavian artery. The left common carotid artery was broken during manipulation. (D) Right subclavian artery originates from the proximal pulmonary trunk, where it bifurcates into the pulmonary arteries. The left pulmonary artery was broken during manipulation.

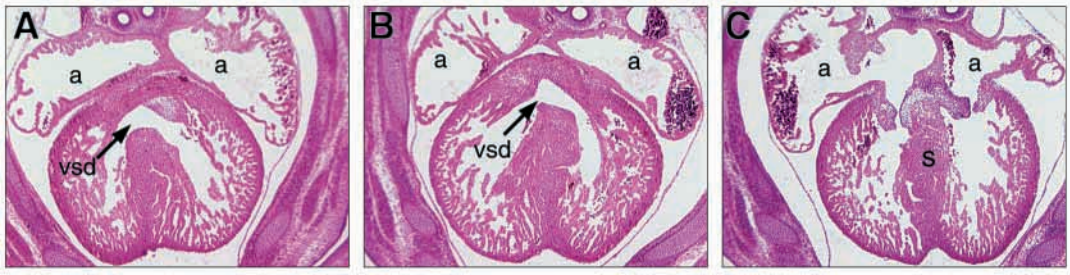

Fig. 7. Ventricular septal defects. (A-C) Transverse sections through hearts of E14.5 PDGFRα$^{fl\Delta/fl\Delta}$;Wnt1Cre^{+} embryos. (A,B) Sections through region of membranous ventricular septum. (C) More caudal section through the heart of embryo in B but containing an intact muscular ventricular septum. a, atrium; s, septum; vsd, ventricular septal defect.

Comparison of NCC conditional embryos and Cre-negative littermate controls at E9.5 revealed no difference in the formation and regression of the first and second arch arteries (Fig. 8D), but when the third, fourth and sixth arteries were examined at E11.5, multiple abnormalities were present in the NCC conditional embryos. In PDGFRα$^{fl/fl}$; Wnt1Cre^{-} embryos, three arch arteries are present on each side, and they have begun to narrow (Fig. 8A). By contrast, the PDGFRα$^{fl/fl}$; Wnt1Cre^{+} embryos exhibited dilated and/or reduced vessels (Fig. 8B,C, and data not shown). Defects were sometimes symmetrical, but often vessels on one side appeared normal, while the other side had severe defects. Deficiencies were observed more frequently on the right side than on the left. Although not as dramatic as the disruptions at E11.5, defects in the fourth and sixth arch arteries could also be identified in E10.5 embryos (data not shown). One surprising feature of this data was the lower penetrance of aortic arch anomalies observed in E17.5-E18.5 embryos compared with the high penetrance of defects observed at E11.5. These data suggest that some resolution of vessel stability may occur at later time points as has been suggested previously (Lindsay and Baldini, 2001).

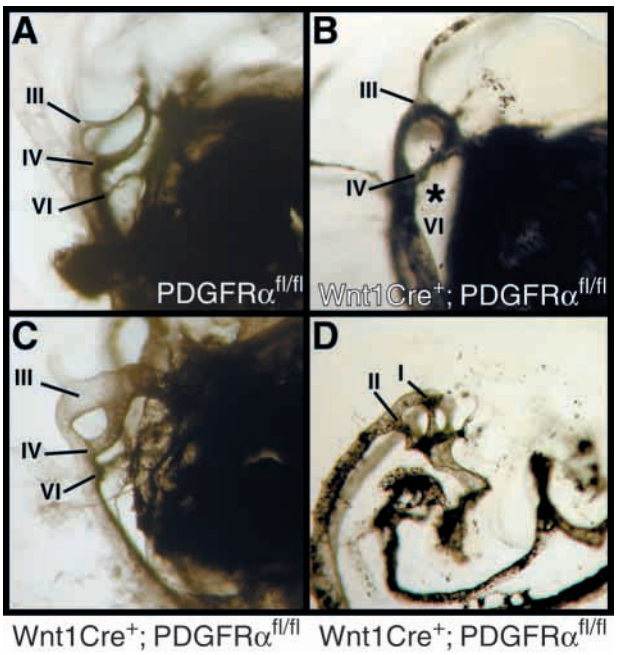

Fig. 8. Vascular anatomy of the branchial arch arteries. (A-D) Intracardiac Indian ink injection of the left ventricle. All images are of the right side of the embryo. (A-C) E11.5 embryos. (D) Normal vessel architecture in a mutant at E9.5. I-IV, first, second, third and fourth branchial arch arteries, respectively; VI, sixth branchial arch artery. *A missing sixth arch artery. In C, the vessels are distended while in the control (A), the vessels have become narrow.

NCC migration and differentiation

As described above, loss of PDGFRα in NCCs does not lead to global deficits in cell proliferation or survival. Because NCCs are a migratory population of cells, we used fate mapping to determine the number and distribution of NCCs as they are moving towards their destinations. For this purpose, PDGFRα$^{fl/fl}$ animals were bred to mice bearing the *R26R* conditional allele described above. PDGFRα$^{fl/fl}$; R26R$^{-/-}$ females were then mated to PDGFR$^{fl/+}$; Wnt1Cre^{+} males. The resulting embryos will have the NCC lineage indelibly marked with β-galactosidase expression (Chai et al., 2000; Jiang et al., 2000). We have examined NCC conditional and littermate control embryos using this technique (Fig. 9). At E9.5, NCC migration can be observed in the cranial, pharyngeal arch and trunk regions (Fig. 9A,B). Mutant embryos were slightly smaller and less mature. Nonetheless, distinct tracts of NCCs can be observed migrating through the somites (Fig. 9B) and nerve tracks can also be discerned. To look specifically at migration of the cardiac crest, we examined transverse section of these embryos through the conotruncal region. NCCs populate the cranial mesenchyme and the pharyngeal arches, as well as migrating along the lateral walls of the aortic sac and truncus arteriosus in both the mutant and control (Fig. 2C,D; Fig. 9C,D). The patterns of migration of tagged NCCs appear very similar. Although a minor reduction in density of NCCs in the pharyngeal arch regions was observed when comparing NCC conditional embryos with littermate controls, this is likely to be due to the maturation stage of the embryo, as more rostral areas such as the first and second pharyngeal arch regions at E9.5 and E10.5 do not exhibit this same reduction (Fig. 2C,D; data not shown). We have also observed mutant and littermate embryos at E13.5 and do not see any major difference in the pattern or intensity of staining even at this later time point (data not shown). These data indicate that PDGFRα-negative NCCs follow the expected paths of migration, and an initial reduction of NCCs in developing tissues is not a likely cause for the defects that we observe in the PDGFRα NCC conditional embryos.

The walls of the vessels of the aortic arch are composed of endothelial cells of mesodermal origin and VSMC of neural crest origin. To determine if the defects observed in the arch arteries was caused by an inability of NCCs to differentiate into VSMC, we analyzed the cellular components of the arch arteries, using immunohistochemistry for detection of vascular endothelial cells and VSMC markers. Cross-sections through the fourth arch artery reveal that both endothelial and VSMC populations appear normal in mutant embryos (Fig. 10). We also analyzed the aortic arch regions for cell proliferation (anti-phospho histone 3) and apoptosis (TUNEL), and saw no difference between mutants and wild types in these assays (data not shown). Taken together, these data indicate that PDGFRα signaling is required for cardiac and cranial NCC development and demonstrate that the developmental defect is likely to be in a subset of NCCs, rather than a global defect or in a PDGFRα-directed cellular response that occurs at a later time point. One possibility is that PDGF regulates cellular functions involved with remodeling of the cranial facial and aortic arch region, such as matrix deposition.

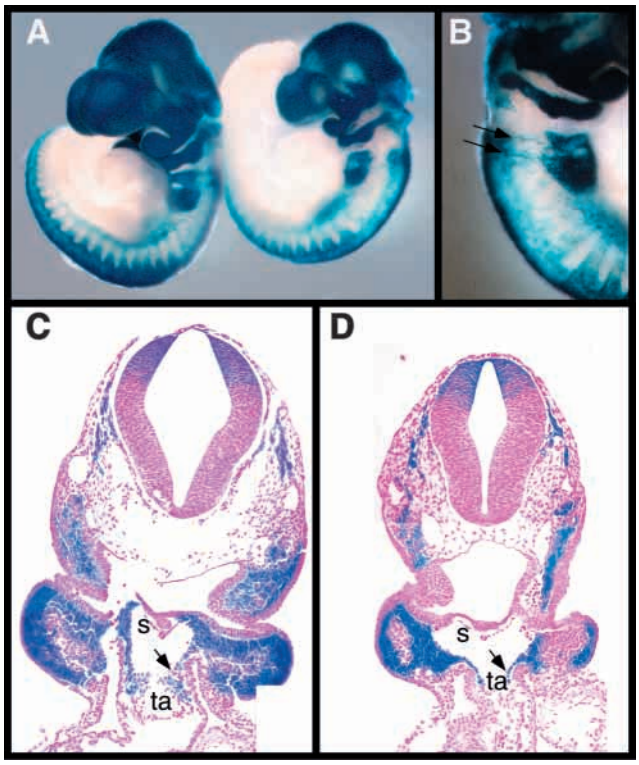

Fig. 9. NCC fate mapping. E9.5 embryos carrying the ROSA26 Cre reporter were stained for β-galactosidase activity. (A,B) Wholemounts. (A, left) PDGFRα$^{fl/+}$;Wnt1Cre^{+}. (A, right) PDGFRα$^{fl/fl}$;Wnt1Cre^{+}. (B) Higher magnification of the migrating NCCs in the PDGFRα$^{fl/fl}$;Wnt1Cre^{+} embryo. Arrows indicate NCCs that have migrated to form part of the peripheral nervous system. (C,D) Transverse sections through conotruncal area of (C) PDGFRα$^{fl/+}$;Wnt1Cre^{+} and (D) PDGFRα$^{fl/fl}$;Wnt1Cre^{+} embryos. Arrows indicate NCCs migrating into the truncus arteriosus. Abbreviations: s, aortic sac; ta, truncus arteriosus.

DISCUSSION

Failure of cranial and cardiac NCCs to migrate and differentiate in their appropriate cellular compartment can result in embryonic defects that in humans are known as velocardiofacial syndrome. While the role of the PDGFRα in these populations of non-neuronal NCCs has been proposed for many years, there has been no conclusive data that the NCC phenotypes observed PDGFRα-deficient embryos were a cell-autonomous phenomenon (Morrison-Graham et al., 1992; Soriano, 1997). The difficulties in understanding the function of this receptor in NCCs originates from the fact the null embryos have a broad range of phenotypes and a high percentage die around E10 (Orr-Urtreger et al., 1992) (M. T. and P. S., unpublished) before NCC populations have begun to differentiate and participate in the formation of the craniofacial and aortic arch ectomesenchyme. Some observations regarding NCC defects have been made previously on *Ph* mutant embryos (Morrison-Graham et al., 1992), but *Ph* is a large deletion encompassing more than the *Pdgfra* gene and the mutation was bred onto another genetic background. This makes it difficult to ascertain that the phenotypes are due to

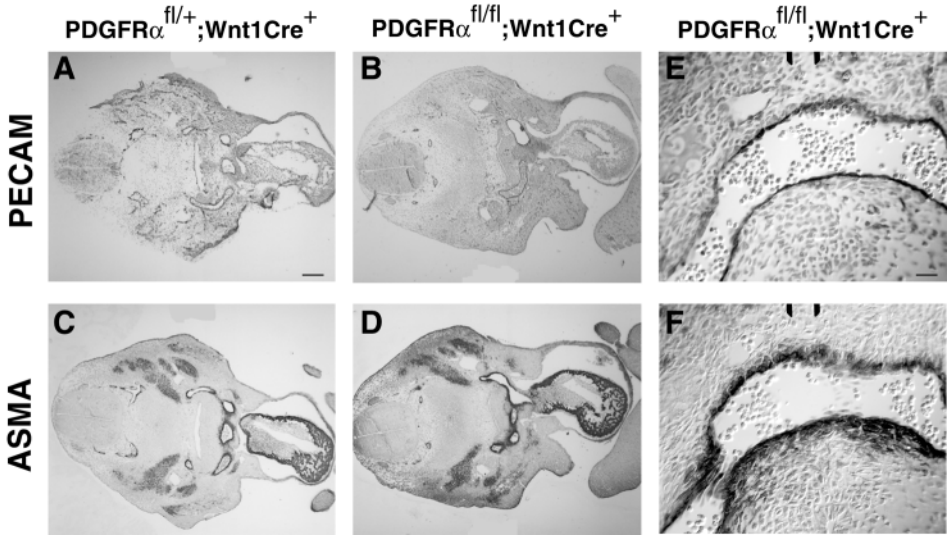

Fig. 10. Mutant arch arteries contain normal numbers of endothelial and VSMC. Transverse sections through fourth arch artery region of E11.5 control (A,C) and mutant (B,D,E,F) embryos. Endothelial and VSMC of the branchial arch arteries were detected using antibodies directed against CD31 (PECAM; A,B,E) and α smooth muscle actin (AMSA; C,D,F), respectively. The higher magnification images (E,F)are from different sections from those shown in B,D to illustrate that vessels appeared normal at many levels. Scale bars: in A, 200 μm for A-D; in E, 25 μm for E,F.

the *Pdgfra* gene alone or to extragenic modifiers. We have used chimeric and conditional analysis to study the role of this pleiotropic gene, and have shown that PDGFRα is directly required in both the cranial and cardiac crest.

Chimeric analysis demonstrated a pronounced selection against null cells in several proliferating areas of mesenchymal cell populations. In fact, wild-type cells predominated in almost every tissue that expresses PDGFRα at high levels (Orr-Urtreger et al., 1992; Orr-Urtreger and Lonai, 1992; Reinertsen et al., 1997; Zhang et al., 1998). These results suggest a cell autonomous requirement for the receptor. Interestingly, there was a simultaneous exclusion of wild-type cells in regions of the head that are derived from paraxial mesoderm. Possibly there is an early localization cue that directs PDGFRα-positive NCCs to cranial mesenchyme, while PDGFRα non-expressing mesoderm is then allocated to the mesodermal core. This is supported by the flow cytometry data from PDGFRα$^{fl/fl}$;Wnt1Cre^{+} branchial arch mesenchyme, where only the NCC population expresses the receptor. The most obvious selection for PDGFRα-expressing cells was in the limb buds and branchial arches. The mutant cells in both tissues were excluded from the distal outgrowth of the mesenchyme, although they were abundant in the ectoderm adjacent to these regions. This pattern of selection has also been observed in chimeras generated with *Fgfr1*- and *Shp2*-null cells (Ciruna et al., 1997; Deng et al., 1997; Saxton et al., 2000). These observations suggest that rapidly proliferating mesenchyme is sensitive to subtle changes in growth factor signaling, resulting in counter-selection of growth factor-deficient cells.

Although no limb development defects are observed in *Pdgfra*$^{-/-}$ embryos, a very pronounced phenotype exists in the NCC-derived cranial bones and cartilage of the nulls. These results are in agreement with the selection in the chimeric embryos and the phenotype in the NCC conditional embryos. Although NCCs require PDGFRα signaling, it is unclear at what stage the signals are essential. The selection in the chimeras occurs very early, based on the paucity of null cells in the mesenchyme of the branchial arches, but the presence of mesenchyme in both the PDGFRα nulls and NCC conditional embryos suggests that the receptor is not absolutely required. Therefore, we propose that PDGFRα may be important at two time points. One may be at the juncture when NCCs are initially populating the arches. At this stage, the PDGFRα would not be essential, but may act synergistically with other growth factor signals to promote NCC proliferation and/or migration. The second time point would be during the morphogenetic processes occurring in the cranial as well as the cardiac regions beginning at E11.5. The PDGFRα would be non-redundant with other pathways at this time, and loss of the signals in NCCs results in the observed phenotypes.

The craniofacial defects observed in the NCC conditional embryos are similar to those described for the *Pdgfra*-null mice. Because only a few null embryos survive to E15-16, the craniofacial malformations associated with the PDGFRα have not been described in depth. Our comparison of E13.5 embryos revealed that the cranial phenotypes in the null embryos were often more severe with regards to the depth of the midline cleft and the amount of hemorrhaging observed. The differences in phenotypes between the null and the NCC conditional can be explained in several ways. The first possibility is that the deletion of the PDGFRα locus in the NCC lineage is incomplete. Therefore, the remaining population of receptor-positive NCCs assuages the defects in the craniofacial mesenchyme. We find this possibility unlikely because the flow cytometry analysis of protein expression in the branchial arch region demonstrated near 100% efficiency of recombination as early as E10.5. A second explanation is that there is a population of later migrating NCCs that never express Wnt1, and therefore never lose PDGFRα expression. The final and most likely explanation is that loss of PDGF signaling in some other cell lineage, possibly somite-derived mesoderm, could also contribute to the severe craniofacial phenotype in the null. Mesoderm cells mix with NCCs and form connective components such as membranes and tendons (Kontges and Lumsden, 1996). Therefore, this population, which is still present in the NCC conditionals, may partially alleviate the null phenotype.

We surmised three possible scenarios for how loss of PDGF signaling results in the observed craniofacial defects. The first could be a direct effect on the primordia of the maxillary region, where PDGFRα would be required for some function such as proliferation, growth or migration. Loss of this signal would lead to a reduction in the number of cranial bone progenitors. Our experiments show that at the initial stages of NCC formation, proliferation, migration and apoptosis are normal in the mutant embryos, suggesting that this simple explanation does not apply to the phenotypes we observe. A second mechanism could be that PDGFRα signals are required to promote the differentiation of CNCC progenitors by mechanisms other than proliferation or cell death, possibly by directing matrix deposition or tissue remodeling. Analysis of NCC ectomesenchyme from *Ph* homozygotes has demonstrated a deficit in metalloprotease 2 (MMP2) (Robbins et al., 1999). Loss of this and similar proteins could affect both NCC migration and frontonasal tissue remodeling. In the third model, PDGFRα may be important for only a subset of cells, rather than affecting the entire cranial and cardiac NCC population. The techniques we have used would only identify global changes in cell number or function. Examination of distinct NCC populations using a variety of markers is currently in progress.

It has been proposed that NCCs contribute to the frontal facial vasculature (Etchevers et al., 2001). Therefore, NCC-derived vascular mural cells (pericytes and VSMC) could fail to populate the frontonasal region, resulting in a disruption of vascular flow or potentially tissue remodeling. In this situation, the mesenchyme might not receive the appropriate signals to mature, resulting in the multiple bone defects that we observe. Supporting this mechanism, a hemorrhage is always present in the frontonasal process and subsequently the nasal capsule in our NCC conditional embryos. Although our data using a pericyte *lacZ* reporter mouse line (Tidhar et al., 2001) indicated no defects in pericytes (data not shown), it is possible that a unique subset of VSMC may be absent or defective. This possibility is currently under investigation.

In addition to the defects in bone and cartilage derived from cranial NCCs, defects in other NCC derivatives in the heart, thymus, teeth and eye have been described in *Ph* and/or *Pdgfra* mutant embryos. The aortic arch defects are readily observable in the NCC conditional embryos, although the penetrance appears to be less than that reported in the *Ph* embryos. The range of defects that we have observed in the NCC conditional

embryos bears a striking resemblance to abnormalities seen in chick cardiac crest ablation experiments (Kirby et al., 1983; Kirby and Waldo, 1990). Although multiple deficiencies were present in the NCC conditional embryos, the most common defects were those concentrated around the conotruncal ridges and aorticopulmonary septum. The fourth and sixth arch arteries contribute to the RSA, ventricular septum and trunk of the arch. Misalignment of the right subclavian artery, ventricular septal defects and persistent truncus arteriosus were often observed in our mutant embryos, while defects of the common carotid and pulmonary arteries were never observed. Therefore, we propose that the PDGFRα, rather than being essential for all cardiac crest, may be important for morphogenesis of the fourth and sixth arch arteries. This hypothesis is supported by the disruptions we observed in the branchial arch arteries earlier in development. It is interesting that the timing of observable defects in cardiac crest cells is the same as that of the craniofacial clefting. In both situations, the NCCs have migrated to their final destination and have adopted a mesenchymal phenotype. The common feature for both tissue populations is that there is a significant amount of cellular rearrangement and tissue remodeling. In the cranial region, the two frontal nasal processes must fuse, while in the aortic arch, multiple vessels are remodeling and/or regressing.

A multitude of mouse mutants have been described with defects in cranial and/or cardiac neural crest derivatives. Clefting of the palate is quite common but the median cleft extending down the forebrain as seen in the PDGFRα mutant embryos is rather rare. This defect results in a virtual absence of the nasal capsule, agenesis of the nasal septum and cleft palate. Similar frontal nasal clefting is seen in transcription factor knockouts (ALX4/Cart double homozygotes) and nuclear receptor knockouts (RARα/γ double homozygotes) (Lohnes et al., 1994; Qu et al., 1999), respectively. How these particular signaling pathways impact one another warrants further investigation.

The most prevalent defect observed in the aortic arch of the NCC conditional embryos is disruption of RSA origin and failure of the conotruncal area to septate. Both of these aortic arch anomalies can be traced back to abnormal development of the fourth arch artery. These disruptions closely resemble those described for haploinsufficiency of the Tbx1 transcription factor that has been implicated in the DiGeorge syndrome phenotypes (Jerome and Papaioannou, 2001; Lindsay et al., 2001; Merscher et al., 2001). Tbx1, however, is expressed in the mesenchyme adjacent to the NCC component of the aortic arch (Garg et al., 2001) and therefore could only interact indirectly with PDGFRα pathway.

We have shown that although the PDGFRα may play an early role in NCC expansion, this role is nonessential. In addition, it is unlikely that the receptor is required for general NCC migration, proliferation or survival. We conclude that the NCC requirement for PDGFRα signaling lies in another cellular function such as differentiation or extracellular matrix deposition, or that PDGFRα action may be on a subset of NCC-derived cells. Loss of the PDGFRα gene exclusively in NCC illustrates an array of defects in both craniofacial and aortic arch development. Our results using both chimeric and conditional analysis conclusively show that the PDGFRα is required cell autonomously in the cranial and cardiac NCC lineages.

We thank Andy McMahon for Wnt1Cre mice, and Philip Corrin, Jason Frazier and Peter Mueting-Nelsen for excellent technical assistance. We also thank Cecilia Moens, Steve Tapscott and our laboratory colleagues for critical reading of the manuscript. M. D. T was the recipient of a fellowship from the American Cancer Society (PF-98-149-01). This work was supported by grants HD24875 and HD25326 from the NIH to P. S.

REFERENCES

Beddington, R. S. and Robertson, E. J. (1989). An assessment of the developmental potential of embryonic stem cells in the midgestation mouse embryo. *Development* **105**, 733-737.

Betsholtz, C., Karlsson, L. and Lindahl, P. (2001). Developmental roles of platelet-derived growth factors. *BioEssays* **23**, 494-507.

Chai, Y., Jiang, X., Ito, Y., Bringas, P., Han, J., Rowitch, D., Soriano, P., McMahon, A. and Sucov, H. (2000). Fate of the mammalian cranial neural crest during tooth and mandibular morphogenesis. *Development* **127**, 1671-1679.

Ciruna, B. G., Schwartz, L., Harpal, K., Yamaguchi, T. P. and Rossant, J. (1997). Chimeric analysis of fibroblast growth factor receptor-1 (Fgfr1) function: a role for FGFR1 in morphogenetic movement through the primitive streak. *Development* **124**, 2829-2841.

Danielian, P. S., Muccino, D., Rowitch, D. H., Michael, S. K. and McMahon, A. P. (1998). Modification of gene activity in mouse embryos in utero by a tamoxifen-inducible form of Cre recombinase. *Curr. Biol.* **8**, 1323-1326.

Deng, C., Bedford, M., Li, C., Xu, X., Yang, X., Dunmore, J. and Leder, P. (1997). Fibroblast growth factor receptor-1 (FGFR-1) is essential for normal neural tube and limb development. *Dev. Biol.* **185**, 42-54.

Echelard, Y., Vassileva, G. and McMahon, A. P. (1994). Cis-acting regulatory sequences governing Wnt-1 expression in the developing mouse CNS. *Development* **120**, 2213-2224.

Etchevers, H. C., Vincent, C., le Douarin, N. M. and Couly, G. F. (2001). The cephalic neural crest provides pericytes and smooth muscle cells to all blood vessels of the face and forebrain. *Development* **128**, 1059-1068.

Friedrich, G. and Soriano, P. (1991). Promoter traps in embryonic stem cells: a genetic screen to identify and mutate developmental genes in mice. *Genes Dev.* **5**, 1513-1523.

Gavalas, A., Trainor, P., Ariza-McNaughton, L. and Krumlauf, R. (2001). Synergy between Hoxa1 and Hoxb1: the relationship between arch patterning and the generation of cranial neural crest. *Development* **128**, 3017-3027.

Garg, V., Yamagishi, C., Hu, T., Kathiriya, I. S., Yamagishi, H. and Srivastava, D. (2001). Tbx1, a DiGeorge syndrome candidate gene, is regulated by sonic hedgehog during pharyngeal arch development. *Dev. Biol.* **235**, 62-73.

Gavrieli, Y., Sherman, Y. and Ben-Sasson, S. A. (1992). Identification of programmed cell death in situ via specific labeling of nuclear DNA fragmentation. *J. Cell Biol.* **119**, 493-501.

Grüneberg, H. and Truslove, G. M. (1960). Two closely linked genes in the mouse. *Genet. Res. Camb.* **1**, 69-90.

Jerome, L. A. and Papaioannou, V. E. (2001). DiGeorge syndrome phenotype in mice mutant for the T-box gene, Tbx1. *Nat. Genet.* **27**, 286-291.

Jiang, X., Rowitch, D., Soriano, P., McMahon, A. and Sucov, H. (2000). Fate of the mammalian cardiac neural crest. *Development* **127**, 1607-1616.

Kirby, M. L., Gale, T. F. and Stewart, D. E. (1983). Neural crest cells contribute to normal aorticopulmonary septation. *Science* **220**, 1059-1061.

Kirby, M. L. and Waldo, K. L. (1990). Role of neural crest in congenital heart disease. *Circulation* **82**, 332-340.

Klinghoffer, R. A., Hamilton, T. G., Hoch, R. and Soriano, P. (2002). An allelic series at the PDGFalphaR locus indicates unequal contributions of distinct signaling pathways during development. *Dev Cell* **2**, 103-113.

Kontges, G. and Lumsden, A. (1996). Rombencephalic neural crest segmentation is preserved throughout craniofaceial ontogeny. *Development* **122**, 3229-3242.

Lindsay, E. A. and Baldini, A. (2001). Recovery from arterial growth delay reduces penetrance of cardiovascular defects in mice deleted for the DiGeorge syndrome region. *Hum. Mol. Genet.* **10**, 997-1002.

Lindsay, E. A., Vitelli, F., Su, H., Morishima, M., Huynh, T., Pramparo,

T., Jurecic, V., Ogunrinu, G., Sutherland, H. F., Scambler, P. J. et al. (2001). Tbx1 haploinsufficieny in the DiGeorge syndrome region causes aortic arch defects in mice. *Nature* **410**, 97-101.

Lohnes, D., Mark, M., Mendelsohn, C., Dolle, P., Dierich, A., Gorry, P., Gansmuller, A. and Chambon, P. (1994). Function of the retinoic acid receptors (RARs) during development (I). Craniofacial and skeletal abnormalities in RAR double mutants. *Development* **120**, 2723-2731.

Maschhoff, K. L. and Baldwin, H. S. (2000). Molecular determinants of neural crest migration. *Am. J. Med. Genet.* **97**, 280-288.

Merscher, S., Funke, B., Epstein, J. A., Heyer, J., Puech, A., Lu, M. M., Xavier, R. J., Demay, M. B., Russell, R. G., Factor, S. et al. (2001). TBX1 is responsible for cardiovascular defects in velo-cardio-facial/DiGeorge syndrome. *Cell* **104**, 619-629.

Morrison-Graham, K., Schatteman, G. C., Bork, T., Bowen-Pope, D. F. and Weston, J. A. (1992). A PDGF receptor mutation in the mouse (Patch) perturbs the development of a non-neuronal subset of neural crest-derived cells. *Development* **115**, 133-142.

Nagy, A. and Rossant, J. (2001). Chimaeras and mosaics for dissecting complex mutant phenotypes. *Int. J. Dev. Biol.* **45**, 577-582.

Orr-Urtreger, A. and Lonai, P. (1992). Platelet-derived growth factor-A and its receptor are expressed in separate, but adjacent cell layers of the mouse embryo. *Development* **115**, 1045-1058.

Orr-Urtreger, A., Bedford, M. T., Do, M. S., Eisenbach, L. and Lonai, P. (1992). Developmental expression of the alpha receptor for platelet-derived growth factor, which is deleted in the embryonic lethal Patch mutation. *Development* **115**, 289-303.

Osumi-Yamashita, N., Ninomiya, Y., Doi, H. and Eto, K. (1994). The contribution of both forebrain and midbrain crest cells to the mesenchyme in the frontonasal mass of mouse embryos. *Dev. Biol.* **164**, 409-419.

Qu, S., Tucker, S., Zhao, Q., deCrombrugghe, B. and Wisdom, R. (1999). Physical and genetic interactions between Alx4 and Cart1. *Development* **126**, 359-369.

Reinertsen, K. K., Bronson, R. T., Stiles, C. D. and Wang, C. (1997). Temporal and spatial specificity of PDGF alpha receptor promoter in transgenic mice. *Gene Expr.* **6**, 301-314.

Robbins, J. R., McGuire, P. G., Wehrle-Haller, B. and Rogers, S. L. (1999). Diminished matrix metalloproteinase 2 (MMP-2) in ectomesenchyme-derived tissues of the Patch mutant mouse: regulation of MMP-2 by PDGF and effects on mesenchymal cell migration. *Dev. Biol.* **212**, 255-263.

Rossant, J. and Spence, A. (1998). Chimeras and mosaics in mouse mutant analysis. *Trends Genet.* **14**, 358-363.

Saxton, T. M., Ciruna, B. G., Holmyard, D., Kulkarni, S., Harpal, K., Rossant, J. and Pawson, T. (2000). The SH2 tyrosine phosphatase shp2 is required for mammalian limb development. *Nat. Genet.* **24**, 420-423.

Schatteman, G. C., Morrison-Graham, K., van Koppen, A., Weston, J. A. and Bowen-Pope, D. F. (1992). Regulation and role of PDGF receptor alpha-subunit expression during embryogenesis. *Development* **115**, 123-131.

Schatteman, G. C., Motley, S. T., Effmann, E. L. and Bowen-Pope, D. F. (1995). Platelet-derived growth factor receptor alpha subunit deleted Patch mouse exhibits severe cardiovascular dysmorphogenesis. *Teratology* **51**, 351-366.

Smith, E. A., Seldin, M. F., Martinez, L., Watson, M. L., Choudhury, G. G., Lalley, P. A., Pierce, J., Aaronson, S., Barker, J., Naylor, S. L. et al. (1991). Mouse platelet-derived growth factor receptor alpha gene is deleted in W19H and patch mutations on chromosome 5. *Proc. Natl. Acad. Sci. USA* **88**, 4811-4815.

Soriano, P. (1997). The PDGF alpha receptor is required for neural crest cell development and for normal patterning of the somites. *Development* **124**, 2691-2700.

Soriano, P. (1999). Generalized lacZ expression with the ROSA26 Cre reporter strain. *Nat. Genet.* **21**, 70-71.

Stephenson, D. A., Mercola, M., Anderson, E., Wang, C. Y., Stiles, C. D., Bowen-Pope, D. F. and Chapman, V. M. (1991). Platelet-derived growth factor receptor alpha-subunit gene (Pdgfra) is deleted in the mouse patch (Ph) mutation. *Proc. Natl. Acad. Sci. USA* **88**, 6-10.

Takakura, N., Yoshida, H., Ogura, Y., Kataoka, H. and Nishikawa, S. (1997). PDGFR alpha expression during mouse embryogenesis: immunolocalization analyzed by whole-mount immunohistostaining using the monoclonal anti-mouse PDGFR alpha antibody APA5. *J. Histochem. Cytochem.* **45**, 883-893.

Tidhar, A., Reichenstein, M., Cohen, D., Faerman, A., Copeland, N. G., Gilbert, D. J., Jenkins, N. A. and Shani, M. (2001). A novel transgenic marker for migrating limb muscle precursors and for vascular smooth muscle cells. *Dev. Dyn.* **220**, 60-73.

Trainor, P. A. and Tam, P. P. (1995). Cranial paraxial mesoderm and neural crest cells of the mouse embryo: co-distribution in the craniofacial mesenchyme but distinct segregation in branchial arches. *Development* **121**, 2569-2582.

Veitch, E., Begbie, J., Schilling, T. F., Smith, M. M. and Graham, A. (1999). Pharyngeal arch patterning in the absence of neural crest. *Curr. Biol.* **9**, 1481-1484.

Zambrowicz, B. P., Imamoto, A., Fiering, S., Herzenberg, L. A., Kerr, W. G. and Soriano, P. (1997). Disruption of overlapping transcripts in the ROSA beta geo 26 gene trap strain leads to widespread expression of beta-galactosidase in mouse embryos and hematopoietic cells. *Proc. Natl. Acad. Sci. USA* **94**, 3789-3794.

Zhang, X. Q., Afink, G. B., Svensson, K., Jacobs, J. J., Gunther, T., Forsberg-Nilsson, K., van Zoelen, E. J., Westermark, B. and Nister, M. (1998). Specific expression in mouse mesoderm- and neural crest-derived tissues of a human PDGFRA promoter/lacZ transgene. *Mech. Dev.* **70**, 167-180.